
Balanced Mixed-Type Tabular Data Synthesis with Diffusion Models

Zeyu Yang¹ Peikun Guo¹ Khadija Zanna¹ Akane Sano¹

Abstract

Diffusion models have emerged as a robust framework for various generative tasks, such as image and audio synthesis, and have also demonstrated a remarkable ability to generate mixed-type tabular data comprising both continuous and discrete variables. However, current approaches to training diffusion models on mixed-type tabular data tend to inherit the imbalanced distributions of features present in the training dataset, which can result in biased sampling. In this research, we introduce a fair diffusion model designed to generate balanced data on sensitive attributes. We present empirical evidence demonstrating that our method effectively mitigates the class imbalance in training data while maintaining the quality of the generated samples. Furthermore, we provide evidence that our approach outperforms existing methods for synthesizing tabular data in terms of performance and fairness.

1. Introduction

Diffusion models (Sohl-Dickstein et al., 2015; Ho et al., 2020) are a class of energy-based generative models utilizing a stochastic process to transform desired data samples from noise iteratively and have demonstrated remarkable performance in generative modeling for various tasks, especially text-to-image synthesis. Researchers use diffusion frameworks to model images paired with text descriptions and show promising results (Nichol et al., 2021; Saharia et al., 2022). Advancing further from diffusion models in pixel space, latent diffusion frameworks optimize image representation in a low-dimensional space, thereby enhancing synthetic image quality and efficiency (Rombach et al., 2022; Ramesh et al., 2022). The impressive results of diffusion models in image synthesis extended to the generation of sequential data such as audio and time series (Kong et al.,

2020; Rasul et al., 2021; Li et al., 2022). This advancement has gradually overshadowed generative adversarial networks (previous research spot in generative modeling), as diffusion models consistently demonstrate superior performance across diverse tasks (Dhariwal & Nichol, 2021; Stypułkowski et al., 2023; Mazé & Ahmed, 2023).

Researchers have recently been motivated by the versatility of diffusion models to explore the potential in synthesizing tabular data (Kotelnikov et al., 2023; He et al., 2023). Tabular data often involves sensitive user information, which raises significant privacy concerns when used for model training. Moreover, such datasets suffer from limitations in size and imbalanced class distribution (Jesus et al., 2022), which leads to challenges in training robust and fair machine learning models. To address these issues, there is a growing demand for effective tabular data synthesis. However, generative modeling of tabular data is challenging due to the combination of discrete and continuous features and their varying value distributions. Interpolation-based techniques, such as SMOTE (Chawla et al., 2002), are simple but effective and challenging to beat. Researchers have used adversarial generative networks and variational autoencoders to generate tabular data with promising results (Ma et al., 2020; Xu et al., 2019). Research on diffusion models for tabular data is ongoing, and the primary challenge is to handle continuous and discrete features simultaneously. In (Austin et al., 2021), the authors suggested using diffusion frameworks for discrete features with Markov transition matrices. Recent developments such as TabDDPM (Kotelnikov et al., 2023), which combines Markov transition functions (called diffusion kernels) for continuous and discrete features, mark significant progress in this field and underscore the potential of diffusion models as a comprehensive solution for tabular data synthesis.

Despite the success of diffusion models in various generative tasks, ethical concerns regarding potential bias and unsafe content in the synthetic data persist. Generative models are inherently data-driven, thereby propagating these biases into the synthetic data. Studies such as (Friedrich et al., 2023; Schramowski et al., 2023) have shown that latent diffusion models, particularly in text-to-image synthesis, can create images biased toward certain privileged groups and may contain inappropriate elements, such as nudity and violence. In response, they propose methods to

¹Department of Electrical and Computer Engineering, Rice University, Houston, USA. Correspondence to: Zeyu Yang <zy45@rice.edu>.

apply hazardous or sensitive guidance in latent space and then eliminate bias and offensive elements in the synthetic images. In addition to text and images, tabular datasets frequently exhibit notable bias, often stemming from issues related to the disproportionate representation of sensitive groups. For instance, some datasets exhibit significant imbalances in demographic groups regarding sensitive attributes such as sex and race (Le Quy et al., 2022). However, in our review of the literature, research on the safety and fairness of diffusion models in areas beyond text-to-image synthesis is limited. Although diffusion models have shown remarkable performance in tabular data synthesis (Sattarov et al., 2023; He et al., 2023; Kotelnikov et al., 2023), they are prone to learning and replicating these biases in training data. To address this issue, we propose a novel diffusion framework to accurately model distributions of mixed-type tabular data, with a specific focus on outcomes and sensitive attributes. We employ balanced sampling techniques to reduce disparities in group representation within the synthetic data. In summary, our main contributions are as follows:

1. We introduce a diffusion-based framework tailored to learn distributions of mixed-type tabular data given multiple attributes.
2. We generate tabular data that is balanced for a predefined set of sensitive attributes, addressing inherent biases in the data.
3. Our model surpasses existing models in specific areas of performance and fairness, as evidenced through comprehensive evaluations.

The remainder of this paper is organized as follows: Section 2 provides an overview of fairness-aware machine learning and diffusion models. Section 3 provides an overview of mixed-type modeling with diffusion models. In Section 4, we detail our approach to multivariate conditioning and balanced sampling. In Section 5, we illustrate the experiments and present the results. Finally, in Section 6, we conclude our findings and discuss their implications.

2. Related Work

The concept of bias in machine learning that involves assigning significance to specific features to enhance overall generalization is essential for the effective performance of models (Mehrabi et al., 2021). However, it is crucial to acknowledge that bias in machine learning can also have negative implications. Negative bias is an inaccurate assumption made by machine learning algorithms that reflects systematic or historical prejudices against certain groups of people (Zanna et al., 2022). Decisions derived from such biased algorithms can lead to adverse effects, particularly impacting specific social groups defined by factors such as

sex, age, disability, race, and more.

This concept of bias and fairness in machine learning has been widely studied, the aim being to mitigate algorithmic bias of sensitive attributes from machine learning models (Mehrabi et al., 2021; Pessach & Shmueli, 2022). Many methods for bias mitigation in classification tasks have been proposed, and they can be classified into three categories: pre-processing, in-processing, and post-processing methods. Pre-processing methods (Kamiran & Calders, 2012; Calmon et al., 2017) transform the collected data to remove discrimination and train machine learning models on discrimination-free datasets. In-processing methods (Zhang et al., 2018; Agarwal et al., 2018; Kamishima et al., 2011; Zafar et al., 2017; Kamishima et al., 2012) regulate machine learning algorithms by incorporating fairness constraints or regularization terms into the objective functions. Lastly, post-processing methods (Hardt et al., 2016; Pleiss et al., 2017), implemented after training machine learning models on collected datasets, directly override the predicted labels to improve fairness. Fairness-aware generative models can be classified as pre-processing methods. In one of such methods proposed to generate fair data, (Xu et al., 2018) introduced fairness-aware adversarial generative networks that employ a fair discriminator to maintain equality in the joint probability of features and labels conditioned on subgroups within sensitive attributes. However, this approach does not effectively tackle the imbalance in sensitive classes within synthetic data, and diffusion-based tabular data synthesis methods such as TabDDPM (Kotelnikov et al., 2023) excel in producing synthetic data of superior quality.

With impressive capabilities in generative modeling, diffusion models are a class of deep generative models that utilize a Markov process that starts from noise and ends with the target data distribution. Although diffusion models are widely studied, the research on fairness and safety of diffusion models is limited, and existing works (Schramowski et al., 2023; Friedrich et al., 2023) mainly focus on text-to-image synthesis tasks. Researchers in (Friedrich et al., 2023) utilize sensitive content, such as sex and race, within text prompts to guide training diffusion models. Subsequently, during the sampling phase, a uniform distribution of sensitive attributes is applied to generate images that are fair and do not exhibit preference towards privileged groups. Similarly, (Schramowski et al., 2023) uses unsafe text, such as nudity and violence, to guide diffusion models and remove unsafe content in the sampling phase. In addition, this method applies some tricks to remove unsafe content from synthetic images while keeping changes minimal. However, these fairness-aware diffusion models have not been adapted to tabular data synthesis, even though bias commonly exists in tabular datasets (Le Quy et al., 2022). This paper studies how to model mixed-type tabular data conditioning on labels and multiple sensitive attributes in latent space.

Our method can generate balanced tabular data considering multiple sensitive attributes and subsequently achieve improved fairness scores without compromising the quality of the synthetic data.

3. Background

Diffusion models, taking inspiration from thermodynamics, are probabilistic generative models that operate under the Markov assumption. Diffusion models involve two major components: a forward process and a reverse process. The forward process gradually transforms the given data \mathbf{x}_0 into noise \mathbf{x}_T passing through T steps of the diffusion kernel $q(\mathbf{x}_t|\mathbf{x}_{t-1})$. In the reverse process, \mathbf{x}_T is restored to the original data \mathbf{x}_0 by T steps of posterior estimator $p_\theta(\mathbf{x}_{t-1}|\mathbf{x}_t)$ with trainable parameters θ . In this section, we explain the Gaussian diffusion kernel for continuous features and the multinomial diffusion kernel for discrete features. Furthermore, we show how to optimize the parameters θ of the posterior estimator considering mixed-type data with both continuous and discrete features.

3.1. Gaussian Diffusion Kernel

The Gaussian diffusion kernel is used in the forward process for continuous features. After a series of Gaussian diffusion kernels with T timesteps, \mathbf{x}_T follows the standard Gaussian distribution $\mathcal{N}(\mathbf{0}, \mathbf{I})$. Specifically, with the values of β_t predefined according to a schedule such as linear, cosine, etc. (Chen, 2023), the Gaussian diffusion kernel $q(\mathbf{x}_t|\mathbf{x}_{t-1})$ can be written as:

$$q(\mathbf{x}_t|\mathbf{x}_{t-1}) = \mathcal{N}(\mathbf{x}_t|\sqrt{1-\beta_t}\mathbf{x}_{t-1}, \beta_t\mathbf{I})$$

With the starting point \mathbf{x}_0 known, the posterior distribution in the forward process can be calculated analytically as follows,

$$\begin{aligned} q(\mathbf{x}_{t-1}|\mathbf{x}_t, \mathbf{x}_0) &= \mathcal{N}(\mathbf{x}_{t-1}|\tilde{\mu}_t(\mathbf{x}_t, \mathbf{x}_0), \tilde{\beta}_t\mathbf{I}) \\ \tilde{\mu}_t(\mathbf{x}_t, \mathbf{x}_0) &= \frac{1}{\sqrt{\alpha_t}}(\mathbf{x}_t - \frac{\beta_t}{\sqrt{1-\alpha_t}}\epsilon) \\ \tilde{\beta}_t &= \frac{1-\bar{\alpha}_{t-1}}{1-\bar{\alpha}_t}\beta_t \end{aligned} \quad (1)$$

where $\alpha_t = 1-\beta_t$, $\bar{\alpha}_t = \prod_{s=1}^t \alpha_s$. In the reverse process, a posterior estimator with parameters θ is used to approximate $p_\theta(\mathbf{x}_{t-1}|\mathbf{x}_t)$ at each timestep t given \mathbf{x}_t .

$$p_\theta(\mathbf{x}_{t-1}|\mathbf{x}_t) = \mathcal{N}(\mathbf{x}_{t-1}|\hat{\mu}(\mathbf{x}_t), \hat{\Sigma}(\mathbf{x}_t))$$

Researchers in (Ho et al., 2020) set the estimated covariance matrix $\hat{\Sigma}(\mathbf{x}_t)$ as diagonal matrix with constant values β_t or $\tilde{\beta}_t$, and calculate the estimated mean $\hat{\mu}(\mathbf{x}_t)$ as follows,

$$\hat{\mu}(\mathbf{x}_t) = \frac{1}{\sqrt{\alpha_t}}(\mathbf{x}_t - \frac{\beta_t}{\sqrt{1-\alpha_t}}\hat{\epsilon}(\mathbf{x}_t)) \quad (2)$$

where $\hat{\epsilon}(\mathbf{x}_t)$ is the estimated noise at time t .

3.2. Multinomial Diffusion Kernel

The multinomial diffusion kernel is applied in the forward process for discrete features with the same noise schedule β_t used by the Gaussian diffusion kernel. For discrete features, in the final timestep T , \mathbf{x}_T follows the discrete uniform distribution $\text{Uniform}(K)$, where K is the number of categories. The multinomial diffusion kernel can be written as:

$$q(\mathbf{x}_t|\mathbf{x}_{t-1}) = \text{Cat}(\mathbf{x}_t|(1-\beta_t)\mathbf{x}_{t-1} + \beta_t/K)$$

Similarly to the continuous case, the posterior distribution of the multinomial diffusion kernel has an analytical solution.

$$q(\mathbf{x}_{t-1}|\mathbf{x}_t, \mathbf{x}_0) = \text{Cat}(\mathbf{x}_{t-1}|\tilde{\theta}/\sum_{k=1}^K \tilde{\theta}_k)$$

$$\tilde{\theta} = [\alpha_t\mathbf{x}_t + (1-\alpha_t)/K] \odot [\bar{\alpha}_{t-1}\mathbf{x}_0 + (1-\bar{\alpha}_{t-1})/K]$$

The posterior estimator for discrete features is preferably parameterized by the estimated starting point $\hat{\mathbf{x}}_0(\mathbf{x}_t)$ as suggested by (Hoogeboom et al., 2021).

$$p_\theta(\mathbf{x}_{t-1}|\mathbf{x}_t) = q(\mathbf{x}_{t-1}|\mathbf{x}_t, \hat{\mathbf{x}}_0(\mathbf{x}_t)) \quad (3)$$

3.3. Model Fitting

The parameters θ of the posterior estimator are learned by minimizing the variational lower bound,

$$\begin{aligned} \mathcal{L}(\mathbf{x}_0) &= \mathbb{E}_{q(\mathbf{x}_0)}[D(q(\mathbf{x}_T|\mathbf{x}_0)||p(\mathbf{x}_T)) - \log p_\theta(\mathbf{x}_0|\mathbf{x}_1) \\ &\quad + \sum_{t=2}^T D(q(\mathbf{x}_{t-1}|\mathbf{x}_t, \mathbf{x}_0)||p_\theta(\mathbf{x}_{t-1}|\mathbf{x}_t))] \end{aligned} \quad (4)$$

where Kullback–Leibler divergence is denoted by D . The variational lower bound can be simplified for continuous variables as the mean squared error between true noise ϵ in Equation (1) and estimated noise $\hat{\epsilon}$ in Equation (2), denoted by \mathcal{L}_G .

$$\mathcal{L}_G = \mathbb{E}_{q(\mathbf{x}_0)}[\|\epsilon - \hat{\epsilon}(\mathbf{x}_t)\|^2]$$

For mixed-type data containing continuous features and C categorical features, the total loss \mathcal{L}_T can be expressed as the summation of the Gaussian diffusion loss term \mathcal{L}_G and the average of the multinomial diffusion loss terms in Equation (4) for all categorical features:

$$\mathcal{L}_T = \mathcal{L}_G + \frac{\sum_{i \leq C} \mathcal{L}^{(i)}}{C}$$

To train latent diffusion models, let \mathbf{z}_t be the latent representation of \mathbf{x}_t , the estimated noise $\hat{\epsilon}(\mathbf{x}_t)$ for continuous features in Equation (2) can be reformulated as $\hat{\epsilon}(\mathbf{z}_t)$. The estimated original input $\hat{\mathbf{x}}_0(\mathbf{x}_t)$ in Equation (3) can be reformulated as $\hat{\mathbf{x}}_0(\mathbf{z}_t)$.

4. Methods

As explained in Section 1, generative diffusion models for tabular data are prone to learning the sensitive group size disparity in training data. In this section, we describe the process of synthesizing balanced mixed-type tabular data considering sensitive attributes. We first introduce conditional generation given multivariate guidance while preserving the synthesis quality. Then, we explain the architecture of the backbone deep neural network used as the posterior estimator in our method. Lastly, we explain the procedure for sampling balanced data with consideration for sensitive attributes. The high-level structure of our method is shown in Figure 1.

4.1. Multivariate Latent Guidance

Conditional data generation is important in many tasks like text-to-image synthesis. To achieve conditional data generation with diffusion models, classifier-free guidance (Ho & Salimans, 2022) is a simple but effective approach. Intuitively, the classifier-free guidance method tries to let the posterior estimator “know” the label of the data it models. In latent space, it uses one neural network to receive \mathbf{z}_t and condition \mathbf{c} to make estimations. We can denote the estimated noise given corresponding condition \mathbf{c} for continuous features as $\bar{\epsilon}(\mathbf{z}_t, \mathbf{c})$,

$$\bar{\epsilon}(\mathbf{z}_t, \mathbf{c}) = \hat{\epsilon}(\mathbf{z}_t) + w_g \underbrace{(\hat{\epsilon}(\mathbf{z}_t, \mathbf{c}) - \hat{\epsilon}(\mathbf{z}_t))}_{\gamma(\mathbf{z}_t, \mathbf{c})} \quad (5)$$

where $\gamma(\mathbf{z}_t, \mathbf{c}) = \hat{\epsilon}(\mathbf{z}_t, \mathbf{c}) - \hat{\epsilon}(\mathbf{z}_t)$ is guidance of \mathbf{c} and it is scaled by guidance weight w_g .

Equation (5) can be extended to support multivariate guidance. Especially in tabular synthesis, we want to generate samples conditioned on labels \mathbf{c} and sensitive features \mathbf{s} . In this case, we can let our neural network take \mathbf{z}_t , \mathbf{c} , and \mathbf{s} as inputs, resulting in:

$$\bar{\epsilon}(\mathbf{z}_t, \mathbf{c}, \mathbf{s}) = \hat{\epsilon}(\mathbf{z}_t) + w_g(\gamma(\mathbf{z}_t, \mathbf{c}) + \gamma(\mathbf{z}_t, \mathbf{c}, \mathbf{s})) \quad (6)$$

$$\gamma(\mathbf{z}_t, \mathbf{c}, \mathbf{s}) = \mu(\mathbf{c}, \mathbf{s}; w_s, \lambda)(\hat{\epsilon}(\mathbf{z}_t, \mathbf{s}) - \hat{\epsilon}(\mathbf{z}_t))$$

The sensitive guidance $\gamma(\mathbf{z}_t, \mathbf{c}, \mathbf{s})$ is controlled elementwisely by a “security gate” $\mu(\mathbf{c}, \mathbf{s}; w_s, \lambda)$,

$$\mu(\mathbf{c}, \mathbf{s}; w_s, \lambda) = \begin{cases} \phi, & \text{where } \hat{\epsilon}(\mathbf{z}_t, \mathbf{c}) \ominus \hat{\epsilon}(\mathbf{z}_t, \mathbf{s}) < \lambda \\ 0, & \text{otherwise} \end{cases}$$

$$\phi = \max(1, w_s |\hat{\epsilon}(\mathbf{z}_t, \mathbf{c}) - \hat{\epsilon}(\mathbf{z}_t, \mathbf{s})|)$$

where w_s is the sensitive guidance weight. The purpose of $\mu(\mathbf{c}, \mathbf{s}; w_s, \lambda)$ is to keep the alterations caused by the sensitive guidance steady and minimal. It deactivates the sensitive guidance when the difference between the estimation conditioned on \mathbf{c} and the estimation conditioned on \mathbf{s} is

larger than a threshold λ . Furthermore, sensitive guidance is deactivated in the early phase of the diffusion process when t is smaller than a warm-up timestep δ (a positive integer indicating the timestep at which sensitive guidance starts):

$$\gamma(\mathbf{z}_t, \mathbf{c}, \mathbf{s}) := \mathbf{0} \text{ if } t < \delta$$

Additionally, a momentum term with momentum weight w_m is added to the sensitivity guidance to make guidance direction stable,

$$\begin{aligned} \gamma_t(\mathbf{z}_t, \mathbf{c}, \mathbf{s}) &= \mu(\mathbf{c}, \mathbf{s}; w_s, \lambda)(\hat{\epsilon}(\mathbf{z}_t, \mathbf{s}) - \hat{\epsilon}(\mathbf{z}_t)) + w_m \nu_t \\ \nu_{t+1} &= \beta \nu_t + (1 - \beta) \gamma_t \end{aligned}$$

where $\nu_0 = \mathbf{0}$ and $\beta \in [0, 1]$. To include not only one sensitive feature, but N sensitive features $\mathbf{S} = \{\mathbf{s}^{(1)}, \dots, \mathbf{s}^{(N)}\}$, we can extend the sensitive guidance as follows:

$$\gamma(\mathbf{z}_t, \mathbf{c}, \mathbf{S}) = \sum_{i=1}^N \mu(\mathbf{c}, \mathbf{s}^{(i)}; w_s, \lambda)(\hat{\epsilon}(\mathbf{z}_t, \mathbf{s}^{(i)}) - \hat{\epsilon}(\mathbf{z}_t))$$

In this way, we can model continuous features given labels \mathbf{c} and a set of sensitive features \mathbf{S} . Similarly, the estimated starting point given \mathbf{c} and \mathbf{S} for discrete features can be formulated as follows,

$$\bar{\mathbf{x}}_0(\mathbf{z}_t, \mathbf{c}, \mathbf{S}) = \hat{\mathbf{x}}_0(\mathbf{z}_t) + w_g(\gamma(\mathbf{z}_t, \mathbf{c}) + \gamma(\mathbf{z}_t, \mathbf{c}, \mathbf{S})) \quad (7)$$

with $\gamma(\mathbf{z}_t, \mathbf{c})$ and $\gamma(\mathbf{z}_t, \mathbf{c}, \mathbf{S})$ parameterized by $\hat{\mathbf{x}}_0$.

4.2. Backbone

In this research, we model mixed-type tabular data in latent space following a similar setup in (Rombach et al., 2022). The tabular data are encoded into latent space and decoded back with multilayer perceptrons. We choose U-Net (Ronneberger et al., 2015) with transformers as a posterior estimator to predict $\bar{\epsilon}(\mathbf{z}_t, \mathbf{c}, \mathbf{S})$ and $\bar{\mathbf{x}}_0(\mathbf{z}_t, \mathbf{c}, \mathbf{S})$. This choice is based on the hypothesis that the U-Net, augmented by the contextual understanding capabilities of transformers, can effectively manage the heterogeneous nature of tabular data. This integration aims to leverage the U-Net’s ability to capture spatial correlation and the transformers’ strengths in sequence modeling, thereby offering a novel approach to latent space modeling of tabular data.

4.3. Balanced Sampling

After training diffusion models on tabular data paired with labels \mathbf{c} and a set of sensitive features \mathbf{S} , we apply multivariate latent guidance for conditional tabular data synthesis. We customize the marginal distributions of the provided labels and sensitive features in the sampling phase. Fair synthetic tabular data are typically anticipated to exhibit the same label distribution as the real data. These data are expected to mirror the label distribution of the real data

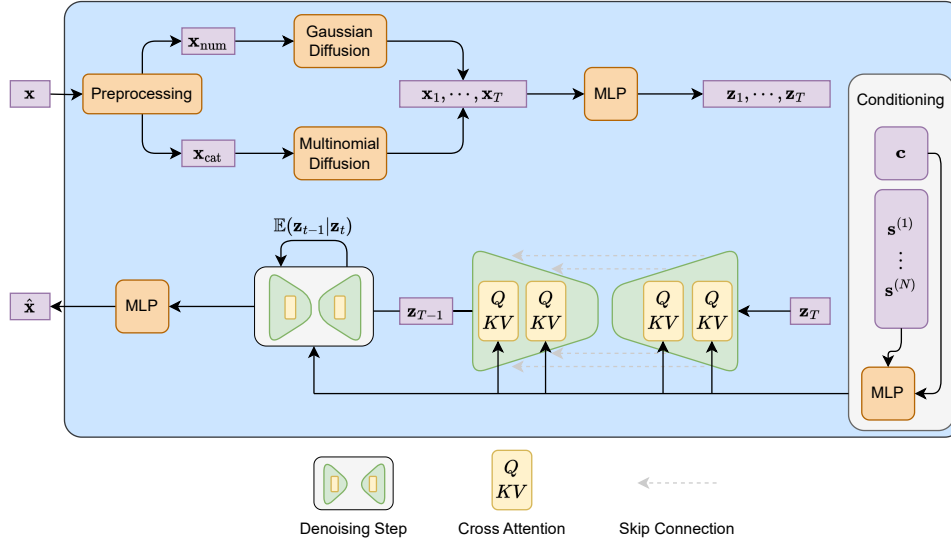


Figure 1. The diagram of our model architecture. In the forward process, the input data point \mathbf{x} is pre-processed into numerical part \mathbf{x}_{num} and categorical part \mathbf{x}_{cat} , and then passing through T steps of the diffusion kernel to get $\mathbf{x}_1, \dots, \mathbf{x}_T$. $\mathbf{z}_1, \dots, \mathbf{z}_T$ is the latent representation of $\mathbf{x}_1, \dots, \mathbf{x}_T$. In the reverse process, the posterior estimator iteratively denoises noisy input \mathbf{z}_T conditioning on an outcome \mathbf{c} and N sensitive attributes $\mathbf{s}^{(1)}, \dots, \mathbf{s}^{(N)}$. The estimated data point is $\hat{\mathbf{x}}$.

and exhibit a balanced distribution of sensitive features, which addresses the common issue of label imbalance in real-world datasets. To achieve this, we can compute the empirical distribution of the labels in the actual data and use it together with uniform categorical distributions for each sensitive feature to guide the sampling process. By doing this, we generate balanced synthetic data regarding the sensitive features, and the synthetic data have the same label distribution as the actual data.

5. Experiments

We first introduce experiment datasets, data processing, baselines, and how we assess synthetic tabular data. Then we present computational results on experimental datasets.

5.1. Datasets

We evaluate the effectiveness and fairness of our proposed method using seven tabular datasets for classification tasks. These datasets contain numerical and categorical features, including some sensitive attributes with observed class imbalances. We provide a summary of the datasets, including their corresponding sensitive attributes in Table 1, and offer further details, such as data sources, sensitive class label distributions, etc., in Appendix A. Common sensitive attributes such as sex and race can be found in data sets like UCI Adult, Cardio, Credit Card, Depression, KDD Census, and Law School. Additionally, other sensitive attributes such as marital status and education are present in the Bank

Marketing and Credit Card datasets. Each data set is divided into training, validation, and test sets using a 50/25/25 split. Following the training of our diffusion models with multivariate guidance, we proceed to generate synthetic data that adheres to the original label distribution while incorporating a uniform distribution for sensitive features.

Table 1. Experimental datasets

| Abbreviation | Dataset | Size | Sensitive | Target |
|--------------|----------------|--------|----------------|--------------|
| AD | UCI Adult | 48842 | Sex, Race | Income |
| BA | Bank Marketing | 45221 | Marital | Subscription |
| CA | Cardio | 70000 | Sex | Diagnosis |
| CR | Credit Card | 30000 | Sex, Education | Payment |
| DE | Depression | 11000 | Sex, Race | Diagnosis |
| KD | KDD Census | 199523 | Sex, Race | Income |
| LA | Law School | 20800 | Sex, Race | Admission |

5.2. Data Processing and Baselines

Data Processing. Following the data processing steps in (Kotelnikov et al., 2023), we split the numerical and categorical features for each dataset and pre-process them separately. Numerical features are converted through quantile transformation, a non-parametric technique transforming variables into a standard Gaussian distribution based on quantiles, thus normalizing the data and enhancing the robustness to outliers. In preparation for the Markov transition process in the latent diffusion model, we encode categorical features into one-hot vectors and concatenate the resulting vectors with normalized numerical features.

Baselines. In assessing the efficacy of our approach for various datasets, we conduct a comparative analysis against several baselines for tabular data synthesis. Within learning-

based methods, we categorize them into diffusion models, generative adversarial networks, and variational autoencoders, selecting the top-performing model from each category with publicly available code. In addition to learning-based techniques, we incorporate SMOTE, a robust and traditional method for tabular data synthesis, into our set of baselines. Specifically, the selected baseline methods for comparison are described in detail as follows.

- **TabDDPM** (Kotelnikov et al., 2023): a recent diffusion-based model that has demonstrated to surpass existing methods for synthesizing tabular data. Leveraging multilayer perceptrons as its backbone, TabDDPM excels in learning unbalanced distributions present in the training data.
- **CTGAN** (Xu et al., 2019): a tabular data synthesis approach based on generative adversarial networks, providing publicly available code that is accessible and user-friendly in (Patki et al., 2016).
- **TVAE** (Xu et al., 2019): a state-of-the-art variational autoencoder specifically designed to generate tabular data with a user-friendly implementation in (Patki et al., 2016).
- **SMOTE** (Chawla et al., 2002): a robust interpolation-based method that creates synthetic data points by combining a real data point with its k nearest neighbors from the dataset. In our application, we leverage SMOTE to generate additional tabular data samples, employing interpolation among existing samples with the same label. The implementation of SMOTE is available in (Lemaître et al., 2017).

5.3. Assessing Synthetic Tabular Data

There are two primary approaches to evaluating synthetic tabular data. One approach is a model-based method that involves training machine learning models on synthetic tabular data and evaluating the trained models on validation data extracted from the original dataset. The other approach is a data-based method that operates independently of machine learning models and directly compares synthetic and real tabular data.

Model-Based Evaluation. The computation procedure of model-based evaluation of synthetic tabular data in classification tasks involves the following steps.

1. Train a generative model on the original training set.
2. Generate synthetic data with the generative model.
3. Train classifiers on the synthetic data.
4. Evaluate classifiers on the original validation data.

Specifically, when assessing model accuracy on the original validation data, it is referred to as **machine learning efficiency** as used in (Choi et al., 2017). Beyond accuracy assessments, the evaluation of synthetic data can extend to fairness scores of classifiers, providing insights into the fairness of the generated data. We evaluate the fairness of machine learning models trained on the synthetic data, focusing on two key aspects: equal allocation and equal performance (Agarwal et al., 2018).

- **Equal allocation**, a fundamental principle in model-based fairness evaluations, entails the idea that a model should distribute resources or opportunities proportionally among different groups, irrespective of their affiliation with any privileged group. Equal allocation is quantified using the **demographic parity ratio**. This ratio reveals the extent of the imbalance by comparing the lowest and highest selection rates (the proportion of examples predicted as positive) between groups.
- **Equal performance** is grounded in the principle that a fair model should exhibit consistent performance across all groups. This entails maintaining the same precision level for each group. The **equalized odds ratio**, which represents the smaller of two ratios comparing true and false positive rates between groups, serves as a metric for assessing performance fairness in this context.

The evaluation of the demographic parity ratio and equalized odds ratio depends on the selection of sensitive features. When evaluating fairness scores in our experiments, we choose the first sensitive feature specified in Table 1. Both the demographic parity ratio and equalized odds ratio are within the range $[0, 1]$. The demographic parity ratio highlights the importance of distributing resources equally among different groups, whereas the equalized odds ratio prioritizes impartial decision-making within each specific group. Higher values in either metric indicate progress toward fairness. However, attaining perfect fairness, represented by a score of 1, may not always be feasible or appropriate depending on the specific context. Our proposed method is expected to have enhanced fairness scores compared to baseline models, and we interpret the results using SHAP feature importance (Lundberg & Lee, 2017).

Data-Based Evaluation. The data-based evaluation directly compares synthetic and real tabular data. To address the privacy concerns when sharing tabular data publicly, the synthetic tabular data is expected not to be a “copy” of the original data. The originality of synthetic data is quantified by utilizing a nearest-neighbor distance metric suggested by (Park et al., 2018), known as the “**distance to the closest record**” (**DCR**), calculated as the Euclidean distance between each synthetic sample and its nearest real data

point. Larger DCR values indicate that the synthetic data has a greater dissimilarity to the original data. In addition, when evaluating the fairness of synthetic tabular data with a data-based method, we examine the imbalance in class characteristics within sensitive features such as sex or race.

5.4. Computational Results

This section presents the computational results of our evaluation of synthetic tabular data generated with five different random seeds. To ensure the robustness of our model-based evaluations, we employed a diverse set of classic classifiers, including decision trees, random forests, support vector machines, multilayer perceptrons, and XGBoost. We determined the optimal model for each synthetic dataset through meticulous training and evaluation across separate training and validation sets, utilizing five random seeds for each model. The averaged validation accuracy, along with the standard deviation, as shown in Table 2, revealed XGBoost as the dominant performer across most datasets, with random forest excelling in one exceptional case (see fairness scores in Appendix A.3).

Table 2. The best and average values of validation accuracy on experimental datasets (the averaged validation accuracy \pm the standard deviation)

| Dataset | Model Choice | Best | Average |
|---------|---------------|-------------------|-------------------|
| AD | XGBoost | 0.866 \pm 0.000 | 0.795 \pm 0.041 |
| BA | XGBoost | 0.900 \pm 0.000 | 0.869 \pm 0.031 |
| CA | XGBoost | 0.733 \pm 0.000 | 0.658 \pm 0.015 |
| CR | Random Forest | 0.816 \pm 0.000 | 0.757 \pm 0.018 |
| DE | XGBoost | 0.941 \pm 0.000 | 0.929 \pm 0.001 |
| KD | XGBoost | 0.956 \pm 0.000 | 0.946 \pm 0.000 |
| LA | XGBoost | 1.000 \pm 0.000 | 0.942 \pm 0.004 |

Performance. In our exploration of the machine learning efficiency of synthetic data compared to baselines, we employ two rigorous protocols. The first protocol calculates the average machine learning efficiency across all classifiers, while the second identifies and utilizes the best classifier for each dataset. This multifaceted approach ensures a robust and insightful evaluation. As illustrated in Table 3, our proposed method maintains competitiveness in terms of average machine learning efficiency, even when incorporating a uniformly distributed direction for sensitive features during the sampling phase. It generally outperforms CTGAN and TVAE. Moreover, our method excels against TabDDPM on the majority of datasets. While the interpolation-based method, SMOTE, proves highly competitive and challenging to outperform, our model achieves a machine learning efficiency very close to SMOTE, underscoring its effectiveness. The best machine learning efficiency exhibits a similar pattern with the average machine learning efficiency, with SMOTE and our model emerging as the two most competitive methods.

Privacy. As explained in Section 5.3, we employ DCR values to assess the privacy score of the synthetic tabular data.

The median DCR values, obtained across five random seeds, are detailed in Table 4. Remarkably, our method consistently attains a superior privacy score in comparison to both SMOTE and TabDDPM. This suggests that our approach excels in maintaining the distinctiveness and privacy of the synthetic data.

Table 4. The median value of distance to the closest record

| | AD | BA | CA | CR | DE | KD | LA |
|---------|-------|-------|-------|-------|-------|-------|-------|
| TabDDPM | 0.179 | 0.195 | 0.021 | 0.123 | 0.520 | 2.089 | 0.176 |
| CTGAN | 0.340 | 0.303 | 0.028 | 0.202 | 0.428 | 2.451 | 0.276 |
| TVAE | 0.253 | 1.415 | 0.032 | 0.208 | 0.443 | 2.018 | 1.414 |
| SMOTE | 0.170 | 0.191 | 0.021 | 0.117 | 0.398 | 2.005 | 0.178 |
| Ours | 0.511 | 0.229 | 0.023 | 0.255 | 0.430 | 2.831 | 0.216 |

Fairness. A key contribution of our work is the generation of balanced tabular data while considering sensitive features. To substantiate our claim and provide empirical evidence, we conduct a thorough assessment of the fairness of our proposed model. After choosing the best-performing classifier for each dataset, we assess its fairness by evaluating two metrics: demographic parity ratio and equalized odds ratio, and the results are presented in Table 5. Our approach outperforms baseline methods notably in terms of equal allocation, as evidenced by higher values of demographic parity ratio across nearly all datasets. For instance, on the KDD Census dataset, our method achieves a demographic parity ratio of 0.613, surpassing baseline methods like SMOTE and TabDDPM by around fifty percent, while SMOTE only attains 0.141, and TabDDPM reaches 0.097. Similarly, on the UCI Adult dataset, our model demonstrates a demographic parity ratio of 0.529, surpassing the ratios of 0.306 by SMOTE and 0.312 by TabDDPM. In addition, our model demonstrates competitiveness in terms of equal performance metrics, as indicated by the equalized odds ratio. Particularly noteworthy are datasets such as UCI Adult and KDD Census, where our model achieves an equalized odds ratio of 0.641 and 0.884, respectively, surpassing baseline models that register less than 0.250 in these metrics. Furthermore, employing equitable synthetic data to train classifiers can yield higher fairness scores compared to training with the original data, as illustrated in Appendix A.3. In contrast, baseline models generally achieve comparable fairness scores.

In Figure 2, we illustrate the feature importance through absolute SHAP values when making predictions with XGBoost on the KDD Census dataset. On the top, we present the scenario where synthetic data generated by our approach exhibits a uniformly distributed sensitive feature, sex, across all samples. In contrast, the figure on the bottom showcases data generated by TabDDPM with biased sampling in the sex feature. It is evident that in the data generated by TabDDPM, the variable sex significantly influences decision-making, while our method mitigates the impact of sex on the final decision to a considerable extent.

Table 3. The values of machine learning efficiency averaged on all types of classifiers

| | Average Accuracy | | | | | | |
|---------|-------------------|-------------------|-------------------|-------------------|-------------------|-------------------|-------------------|
| | AD | BA | CA | CR | DE | KD | LA |
| TabDDPM | 0.777 \pm 0.093 | 0.874 \pm 0.017 | 0.640 \pm 0.025 | 0.768 \pm 0.032 | 0.920 \pm 0.001 | 0.937 \pm 0.001 | 0.905 \pm 0.012 |
| CTGAN | 0.742 \pm 0.148 | 0.873 \pm 0.019 | 0.600 \pm 0.061 | 0.746 \pm 0.058 | 0.867 \pm 0.050 | 0.931 \pm 0.014 | 0.882 \pm 0.112 |
| TVAE | 0.786 \pm 0.023 | 0.854 \pm 0.026 | 0.613 \pm 0.058 | 0.784 \pm 0.021 | 0.881 \pm 0.051 | 0.938 \pm 0.008 | 0.919 \pm 0.119 |
| SMOTE | 0.807 \pm 0.038 | 0.880 \pm 0.022 | 0.632 \pm 0.074 | 0.770 \pm 0.044 | 0.928 \pm 0.022 | 0.939 \pm 0.013 | 0.930 \pm 0.124 |
| Ours | 0.803 \pm 0.022 | 0.880 \pm 0.011 | 0.629 \pm 0.001 | 0.734 \pm 0.045 | 0.926 \pm 0.004 | 0.932 \pm 0.004 | 0.921 \pm 0.003 |
| | Best Accuracy | | | | | | |
| | AD | BA | CA | CR | DE | KD | LA |
| TabDDPM | 0.834 \pm 0.004 | 0.895 \pm 0.003 | 0.708 \pm 0.003 | 0.816 \pm 0.002 | 0.937 \pm 0.003 | 0.945 \pm 0.001 | 0.964 \pm 0.002 |
| CTGAN | 0.817 \pm 0.002 | 0.888 \pm 0.002 | 0.652 \pm 0.006 | 0.716 \pm 0.009 | 0.870 \pm 0.008 | 0.941 \pm 0.001 | 0.975 \pm 0.002 |
| TVAE | 0.810 \pm 0.004 | 0.849 \pm 0.008 | 0.662 \pm 0.006 | 0.773 \pm 0.006 | 0.900 \pm 0.003 | 0.944 \pm 0.001 | 0.993 \pm 0.001 |
| SMOTE | 0.853 \pm 0.000 | 0.898 \pm 0.000 | 0.704 \pm 0.000 | 0.817 \pm 0.001 | 0.941 \pm 0.000 | 0.949 \pm 0.000 | 1.000 \pm 0.000 |
| Ours | 0.838 \pm 0.001 | 0.892 \pm 0.003 | 0.709 \pm 0.004 | 0.806 \pm 0.004 | 0.942 \pm 0.003 | 0.930 \pm 0.003 | 0.995 \pm 0.004 |

Table 5. The values of demographic parity ratio and equalized odds ratio with the best-performing classifier

| | Demographic Parity Ratio | | | | | | |
|---------|--------------------------|-------------------|-------------------|-------------------|-------------------|-------------------|-------------------|
| | AD | BA | CA | CR | DE | KD | LA |
| TabDDPM | 0.312 \pm 0.033 | 0.590 \pm 0.070 | 0.957 \pm 0.036 | 0.791 \pm 0.063 | 0.634 \pm 0.020 | 0.097 \pm 0.032 | 0.858 \pm 0.007 |
| TabGAN | 0.188 \pm 0.039 | 0.749 \pm 0.060 | 0.760 \pm 0.027 | 0.915 \pm 0.051 | 0.706 \pm 0.021 | 0.112 \pm 0.037 | 0.844 \pm 0.006 |
| TabVAE | 0.249 \pm 0.017 | 0.624 \pm 0.045 | 0.965 \pm 0.011 | 0.740 \pm 0.088 | 0.664 \pm 0.012 | 0.092 \pm 0.027 | 0.847 \pm 0.006 |
| SMOTE | 0.306 \pm 0.000 | 0.625 \pm 0.000 | 0.975 \pm 0.000 | 0.787 \pm 0.000 | 0.671 \pm 0.000 | 0.141 \pm 0.000 | 0.851 \pm 0.000 |
| Ours | 0.529 \pm 0.046 | 0.839 \pm 0.098 | 0.963 \pm 0.017 | 0.828 \pm 0.048 | 0.706 \pm 0.005 | 0.613 \pm 0.057 | 0.862 \pm 0.007 |
| | Equalized Odds Ratio | | | | | | |
| | AD | BA | CA | CR | DE | KD | LA |
| TabDDPM | 0.247 \pm 0.033 | 0.496 \pm 0.077 | 0.919 \pm 0.068 | 0.680 \pm 0.081 | 0.764 \pm 0.110 | 0.134 \pm 0.050 | 0.593 \pm 0.484 |
| CTGAN | 0.125 \pm 0.047 | 0.760 \pm 0.074 | 0.669 \pm 0.038 | 0.895 \pm 0.048 | 0.815 \pm 0.062 | 0.178 \pm 0.067 | 0.611 \pm 0.172 |
| TVAE | 0.205 \pm 0.023 | 0.621 \pm 0.046 | 0.950 \pm 0.027 | 0.667 \pm 0.115 | 0.825 \pm 0.067 | 0.126 \pm 0.046 | 0.562 \pm 0.175 |
| SMOTE | 0.231 \pm 0.000 | 0.593 \pm 0.000 | 0.939 \pm 0.000 | 0.683 \pm 0.000 | 0.827 \pm 0.000 | 0.202 \pm 0.000 | 1.000 \pm 0.000 |
| Ours | 0.641 \pm 0.108 | 0.760 \pm 0.043 | 0.901 \pm 0.035 | 0.802 \pm 0.056 | 0.254 \pm 0.089 | 0.884 \pm 0.055 | 0.170 \pm 0.340 |

Apart from fairness evaluation dependent on machine learning models, we also analyze the class distribution within the sensitive attributes. For example, in the UCI Adult dataset, the distribution of sensitive attributes has an inherent bias. In contrast, the synthetic data generated through our approach exhibits more balanced distributions, as depicted in Figure 3, where the y-axis represents the percentage of the respective attribute. We present visualizations of class imbalance in sensitive attributes for the rest of experimental datasets in Figure 4.

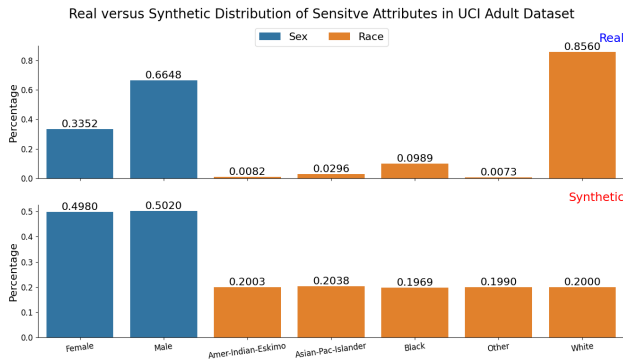


Figure 3. Comparison in the real vs. synthetic distribution of sensitive attributes in the UCI Adult dataset

5.5. Limitations and Discussion

Our proposed method is designed to generate balanced synthetic tabular data considering sensitive attributes. Empiri-

cally, classifiers trained on such balanced synthetic tabular data demonstrate higher fairness scores at equal allocation metrics indicated by demographic parity ratios. However, there is no guarantee that equal performance, reflected by equalized odds ratios, will always improve. We use U-Net with attention layers as the backbone neural network for the posterior estimator in the diffusion framework, but it is time-consuming. Despite our model exhibiting superior machine learning efficiency and higher fairness scores compared to other deep generative models in our experiments, the computational time is approximately five times longer. In the future, we may explore the incorporation of constraints to ensure equal performance and seek ways to reduce computational costs.

6. Conclusion

In this work, we propose a novel diffusion model framework for mixed-type tabular data conditioned on both outcome and sensitive feature variables. Our approach leverages a multivariate guidance mechanism and performs balanced sampling considering sensitive features while ensuring a fair representation of the generated data. Extensive experiments on real-world datasets containing sensitive demographics demonstrate that our model achieves competitive performance and superior fairness compared to existing baselines.

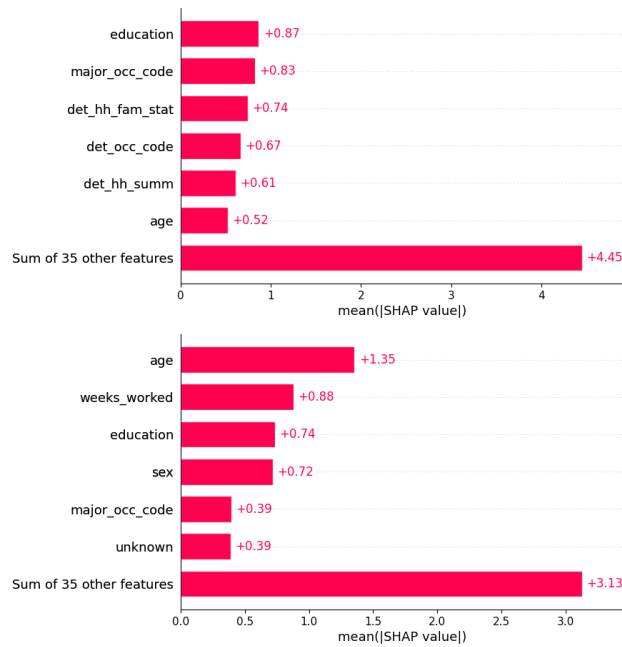


Figure 2. Comparison in SHAP values on KDD dataset: balanced scenario (top) vs. unbalanced scenario (bottom) using XGBoost

Impact Statements

The objective of this study is to make progress in the area of fair machine learning. Tabular datasets sometimes contain inherent bias, such as imbalanced distributions in sensitive attributes. Training machine learning models on biased datasets may result in decisions that could negatively affect minority groups. By mitigating biases present in tabular datasets through the generation of equitable synthetic data, our approach contributes to fostering equitable decision-making processes across industries such as finance, healthcare, and employment. Moreover, in instances where sharing datasets becomes necessary, the utilization of fair synthetic data ensures the preservation of user privacy and avoids causing emotional distress to minority groups. An adverse possibility is that bad individuals could manipulate distributions in sensitive attributes to generate biased (even stronger than original) data to harm minority groups.

References

Agarwal, A., Beygelzimer, A., Dudík, M., Langford, J., and Wallach, H. A reductions approach to fair classification. In *International conference on machine learning*, pp. 60–69. PMLR, 2018.

Austin, J., Johnson, D. D., Ho, J., Tarlow, D., and Van Den Berg, R. Structured denoising diffusion models in discrete state-spaces. *Advances in Neural Information Processing Systems*, 34:17981–17993, 2021.

Borisov, V., Leemann, T., Seßler, K., Haug, J., Pawelczyk, M., and Kasneci, G. Deep neural networks and tabular data: A survey. *IEEE Transactions on Neural Networks and Learning Systems*, 2022.

Calmon, F., Wei, D., Vinzamuri, B., Natesan Ramamurthy, K., and Varshney, K. R. Optimized pre-processing for discrimination prevention. *Advances in neural information processing systems*, 30, 2017.

Chawla, N. V., Bowyer, K. W., Hall, L. O., and Kegelmeyer, W. P. Smote: synthetic minority over-sampling technique. *Journal of artificial intelligence research*, 16:321–357, 2002.

Chen, T. On the importance of noise scheduling for diffusion models. *arXiv preprint arXiv:2301.10972*, 2023.

Choi, E., Biswal, S., Malin, B., Duke, J., Stewart, W. F., and Sun, J. Generating multi-label discrete patient records using generative adversarial networks. In *Machine learning for healthcare conference*, pp. 286–305. PMLR, 2017.

Dhariwal, P. and Nichol, A. Diffusion models beat gans on image synthesis. *Advances in neural information processing systems*, 34:8780–8794, 2021.

Friedrich, F., Schramowski, P., Brack, M., Struppek, L., Hintersdorf, D., Luccioni, S., and Kersting, K. Fair diffusion: Instructing text-to-image generation models on fairness. *arXiv preprint arXiv:2302.10893*, 2023.

Hardt, M., Price, E., and Srebro, N. Equality of opportunity in supervised learning. *Advances in neural information processing systems*, 29, 2016.

He, H., Zhao, S., Xi, Y., and Ho, J. C. Meddiff: Generating electronic health records using accelerated denoising diffusion model. *arXiv preprint arXiv:2302.04355*, 2023.

Ho, J. and Salimans, T. Classifier-free diffusion guidance. *arXiv preprint arXiv:2207.12598*, 2022.

Ho, J., Jain, A., and Abbeel, P. Denoising diffusion probabilistic models. *Advances in neural information processing systems*, 33:6840–6851, 2020.

Hoogeboom, E., Nielsen, D., Jaini, P., Forré, P., and Welling, M. Argmax flows and multinomial diffusion: Learning categorical distributions. *Advances in Neural Information Processing Systems*, 34:12454–12465, 2021.

Jesus, S., Pombal, J., Alves, D., Cruz, A., Saleiro, P., Ribeiro, R., Gama, J., and Bizarro, P. Turning the tables: Biased, imbalanced, dynamic tabular datasets for ml evaluation. *Advances in Neural Information Processing Systems*, 35:33563–33575, 2022.

- Kamiran, F. and Calders, T. Data preprocessing techniques for classification without discrimination. *Knowledge and information systems*, 33(1):1–33, 2012.
- Kamishima, T., Akaho, S., and Sakuma, J. Fairness-aware learning through regularization approach. In *2011 IEEE 11th International Conference on Data Mining Workshops*, pp. 643–650. IEEE, 2011.
- Kamishima, T., Akaho, S., Asoh, H., and Sakuma, J. Fairness-aware classifier with prejudice remover regularizer. In *Machine Learning and Knowledge Discovery in Databases: European Conference, ECML PKDD 2012, Bristol, UK, September 24-28, 2012. Proceedings, Part II* 23, pp. 35–50. Springer, 2012.
- Kohavi, R. et al. Scaling up the accuracy of naive-bayes classifiers: A decision-tree hybrid. In *Kdd*, volume 96, pp. 202–207, 1996.
- Kong, Z., Ping, W., Huang, J., Zhao, K., and Catanzaro, B. Diffwave: A versatile diffusion model for audio synthesis. *arXiv preprint arXiv:2009.09761*, 2020.
- Kotelnikov, A., Baranchuk, D., Rubachev, I., and Babenko, A. Tabddpm: Modelling tabular data with diffusion models. In *International Conference on Machine Learning*, pp. 17564–17579. PMLR, 2023.
- Le Quy, T., Roy, A., Iosifidis, V., Zhang, W., and Ntoutsi, E. A survey on datasets for fairness-aware machine learning. *Wiley Interdisciplinary Reviews: Data Mining and Knowledge Discovery*, 12(3):e1452, 2022.
- Lemaître, G., Nogueira, F., and Aridas, C. K. Imbalanced-learn: A python toolbox to tackle the curse of imbalanced datasets in machine learning. *Journal of machine learning research*, 18(17):1–5, 2017.
- Li, Y., Lu, X., Wang, Y., and Dou, D. Generative time series forecasting with diffusion, denoise, and disentanglement. *Advances in Neural Information Processing Systems*, 35: 23009–23022, 2022.
- Lundberg, S. M. and Lee, S.-I. A unified approach to interpreting model predictions. *Advances in neural information processing systems*, 30, 2017.
- Ma, C., Tschitschek, S., Turner, R., Hernández-Lobato, J. M., and Zhang, C. Vaem: a deep generative model for heterogeneous mixed type data. *Advances in Neural Information Processing Systems*, 33:11237–11247, 2020.
- Mazé, F. and Ahmed, F. Diffusion models beat gans on topology optimization. In *Proceedings of the AAAI Conference on Artificial Intelligence (AAAI), Washington, DC*, 2023.
- Mehrabi, N., Morstatter, F., Saxena, N., Lerman, K., and Galstyan, A. A survey on bias and fairness in machine learning. *ACM computing surveys (CSUR)*, 54(6):1–35, 2021.
- Nichol, A., Dhariwal, P., Ramesh, A., Shyam, P., Mishkin, P., McGrew, B., Sutskever, I., and Chen, M. Glide: Towards photorealistic image generation and editing with text-guided diffusion models. *arXiv preprint arXiv:2112.10741*, 2021.
- Park, N., Mohammadi, M., Gorde, K., Jajodia, S., Park, H., and Kim, Y. Data synthesis based on generative adversarial networks. *arXiv preprint arXiv:1806.03384*, 2018.
- Patki, N., Wedge, R., and Veeramachaneni, K. The synthetic data vault. In *2016 IEEE International Conference on Data Science and Advanced Analytics (DSAA)*, pp. 399–410. IEEE, 2016.
- Pessach, D. and Shmueli, E. A review on fairness in machine learning. *ACM Computing Surveys (CSUR)*, 55(3):1–44, 2022.
- Pleiss, G., Raghavan, M., Wu, F., Kleinberg, J., and Weinberger, K. Q. On fairness and calibration. *Advances in neural information processing systems*, 30, 2017.
- Ramesh, A., Dhariwal, P., Nichol, A., Chu, C., and Chen, M. Hierarchical text-conditional image generation with clip latents. *arXiv preprint arXiv:2204.06125*, 1(2):3, 2022.
- Rasul, K., Seward, C., Schuster, I., and Vollgraf, R. Autoregressive denoising diffusion models for multivariate probabilistic time series forecasting. In *International Conference on Machine Learning*, pp. 8857–8868. PMLR, 2021.
- Rombach, R., Blattmann, A., Lorenz, D., Esser, P., and Ommer, B. High-resolution image synthesis with latent diffusion models. In *Proceedings of the IEEE/CVF conference on computer vision and pattern recognition*, pp. 10684–10695, 2022.
- Ronneberger, O., Fischer, P., and Brox, T. U-net: Convolutional networks for biomedical image segmentation. In *Medical Image Computing and Computer-Assisted Intervention—MICCAI 2015: 18th International Conference, Munich, Germany, October 5-9, 2015, Proceedings, Part III* 18, pp. 234–241. Springer, 2015.
- Saharia, C., Chan, W., Saxena, S., Li, L., Whang, J., Denton, E. L., Ghasemipour, K., Gontijo Lopes, R., Karagol Ayan, B., Salimans, T., et al. Photorealistic text-to-image diffusion models with deep language understanding. *Advances in Neural Information Processing Systems*, 35: 36479–36494, 2022.

- Sattarov, T., Schreyer, M., and Borth, D. Findiff: Diffusion models for financial tabular data generation. In *Proceedings of the Fourth ACM International Conference on AI in Finance*, pp. 64–72, 2023.
- Schramowski, P., Brack, M., Deiseroth, B., and Kersting, K. Safe latent diffusion: Mitigating inappropriate degeneration in diffusion models. In *Proceedings of the IEEE/CVF Conference on Computer Vision and Pattern Recognition*, pp. 22522–22531, 2023.
- Sohl-Dickstein, J., Weiss, E., Maheswaranathan, N., and Ganguli, S. Deep unsupervised learning using nonequilibrium thermodynamics. In *International conference on machine learning*, pp. 2256–2265. PMLR, 2015.
- Stypułkowski, M., Vougioukas, K., He, S., Zieba, M., Petridis, S., and Pantic, M. Diffused heads: Diffusion models beat gans on talking-face generation. *arXiv preprint arXiv:2301.03396*, 2023.
- Xu, D., Yuan, S., Zhang, L., and Wu, X. Fairgan: Fairness-aware generative adversarial networks. In *2018 IEEE International Conference on Big Data (Big Data)*, pp. 570–575. IEEE, 2018.
- Xu, L., Skoularidou, M., Cuesta-Infante, A., and Veeramachaneni, K. Modeling tabular data using conditional gan. *Advances in neural information processing systems*, 32, 2019.
- Yeh, I.-C. and Lien, C.-h. The comparisons of data mining techniques for the predictive accuracy of probability of default of credit card clients. *Expert systems with applications*, 36(2):2473–2480, 2009.
- Zafar, M. B., Valera, I., Ródriguez, M. G., and Gummadi, K. P. Fairness constraints: Mechanisms for fair classification. In *Artificial intelligence and statistics*, pp. 962–970. PMLR, 2017.
- Zanna, K., Sridhar, K., Yu, H., and Sano, A. Bias reducing multitask learning on mental health prediction. In *2022 10th International Conference on Affective Computing and Intelligent Interaction (ACII)*, pp. 1–8. IEEE, 2022.
- Zhang, B. H., Lemoine, B., and Mitchell, M. Mitigating unwanted biases with adversarial learning. In *Proceedings of the 2018 AAAI/ACM Conference on AI, Ethics, and Society*, pp. 335–340, 2018.
- Zhang, C., Zhang, C., Zhang, M., and Kweon, I. S. Text-to-image diffusion model in generative ai: A survey. *arXiv preprint arXiv:2303.07909*, 2023.

A. Details about Datasets

A.1. Data Sources

A.1.1. UCI ADULT

The UCI Adult dataset (Kohavi et al., 1996) is widely used as a benchmark for exploring fairness and bias in machine learning. It contains 48842 data points. Each data point has 14 attributes and a binary target variable indicating whether an individual earns over fifty thousand dollars annually. The dataset encompasses employment, education, and demographic information, and sensitive features are sex and race. Download it from [OpenML](#).

A.1.2. BANK MARKETING

The Bank Marketing dataset is collected from direct marketing campaigns of a Portuguese banking institution. Comprising 45211 instances with 16 features, the predicted outcome is a binary variable indicating whether a client subscribed to a term deposit. Demographic, economic, and past marketing campaign data are included in features, and marital status is sensitive. Download it from [OpenML](#).

A.1.3. CARDIO

The Cardio dataset focuses on diagnosing cardiovascular disease (yes or no) and it contains 70000 instances. It incorporates 11 features, which contain demographics and factual information (blood pressure, cholesterol levels, etc.), as well as self-reported labels such as whether smoking or not. The sensitive feature is sex. Download it from [OpenML](#).

A.1.4. CREDIT CARD

The Credit Card dataset (Yeh & Lien, 2009) explores customer default payments (yes or no) among credit card clients in Taiwan, and it contains 30000 data points. Each data point has 23 features including the information of demographics and financial records (monthly payments, etc.). The sensitive features are sex and education. Download it from [OpenML](#).

A.1.5. DEPRESSION

The Depression dataset contains demographic and clinical data (concentration, rumination, etc.) to predict a diagnosis of depression. It has 11000 instances, each with 18 features, and sensitive features are sex and race. Download it from [OpenML](#).

A.1.6. KDD CENSUS

The KDD Census dataset is an expanded version of the UCI Adult dataset. It involves 199523 instances, each featuring 41 attributes and a binary target variable indicating income over fifty thousand dollars per year. The dataset covers employment, education, and demographic details, with sex and race as sensitive features. Download it from [OpenML](#).

A.1.7. LAW SCHOOL

The Law School dataset presents a survey on the law school admission process. It has 20800 instances. Each instance has 12 attributes and a binary target variable indicating admission to law school. Demographic and academic information, such as GPA, are included in features. The sensitive features are sex and race. Download it from [OpenML](#).

A.2. Number of Features

| Dataset | Number of Numerical Features | Number of Categorical Features |
|----------------|------------------------------|--------------------------------|
| UCI Adult | 6 | 8 |
| Bank Marketing | 7 | 9 |
| Cardio | 5 | 6 |
| Credit Card | 14 | 9 |
| Depression | 14 | 4 |
| KDD Census | 7 | 34 |
| Law School | 6 | 6 |

Table 6. The number of numerical attributes and categorical attributes in experimental datasets

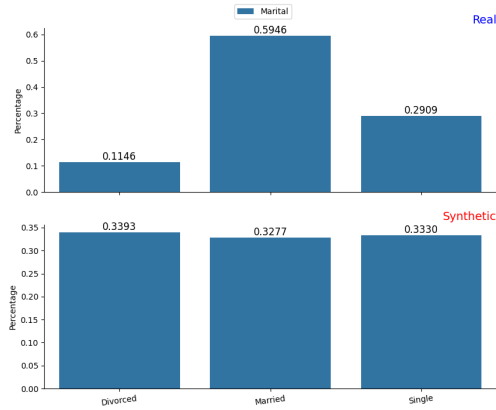
A.3. Evaluation of Best-Performing Classifiers on Original Datasets

| Dataset | Model Choice | Accuracy | Demographic Parity Ratio | Equalized Odds Ratio |
|----------------|---------------|----------|--------------------------|----------------------|
| UCI Adult | XGBoost | 0.866 | 0.353 | 0.273 |
| Bank Marketing | XGBoost | 0.900 | 0.619 | 0.540 |
| Cardio | XGBoost | 0.733 | 0.992 | 0.989 |
| Credit Card | Random Forest | 0.816 | 0.778 | 0.834 |
| Depression | XGBoost | 0.941 | 0.696 | 0.644 |
| KDD Census | XGBoost | 0.956 | 0.151 | 0.170 |
| Law School | XGBoost | 1.000 | 0.825 | 1.000 |

Table 7. The values of accuracy and fairness scores of the best-performing classifier on experimental datasets

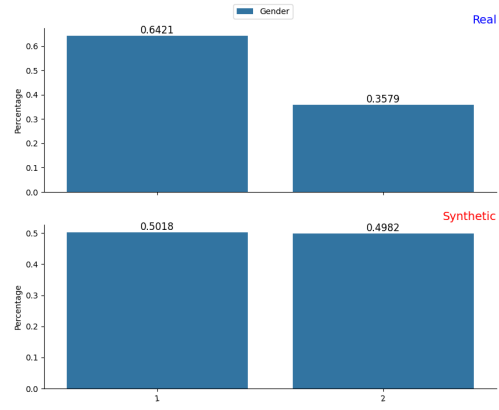
A.4. Class Imbalance

Real versus Synthetic Distribution of Sensitive Attributes in Bank Marketing Dataset



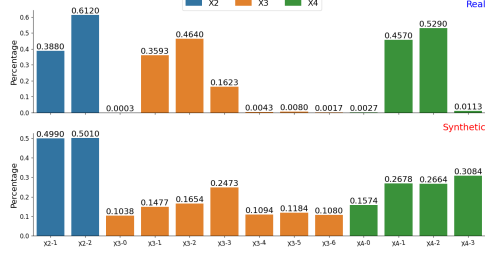
(a) Bank Marketing

Real versus Synthetic Distribution of Sensitive Attributes in Cardio Dataset



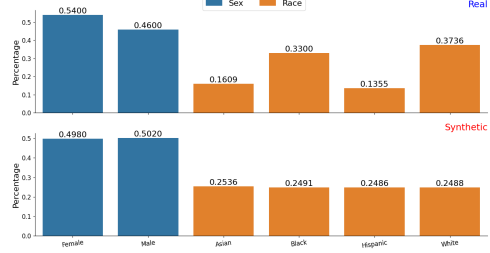
(b) Cardio

Real versus Synthetic Distribution of Sensitive Attributes in Credit Card Dataset



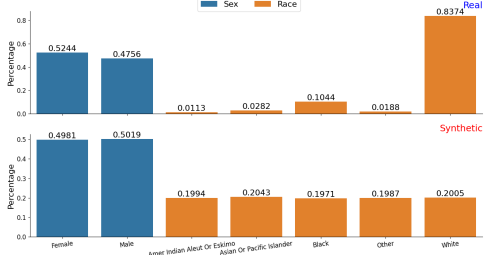
(c) Credit Card

Real versus Synthetic Distribution of Sensitive Attributes in Depression Dataset



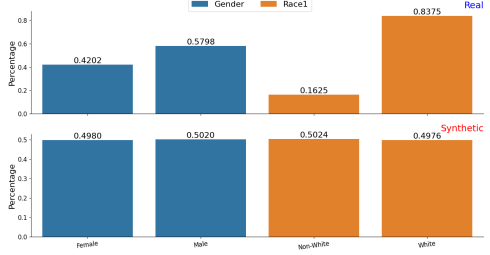
(d) Depression

Real versus Synthetic Distribution of Sensitive Attributes in KDD Census Dataset



(e) KDD Census

Real versus Synthetic Distribution of Sensitive Attributes in Law School Dataset



(f) Law School

Figure 4. Visualizations of class imbalance in sensitive attributes in experimental datasets except UCI Adult